Atomic-level investigation of the growth of Si/Ge by ultrahigh vacuum chemical vapor deposition

D.-S. Lin
Institute of Physics, National Chiao-Tung University, Hsinchu, Taiwan, Republic of China

T. Miller and T.-C. Chiang[a)]
Department of Physics and Materials Research Laboratory, University of Illinois, Urbana, Illinois 61801

(Received 25 September 1996; accepted 17 February 1997)

Si and Ge films can be prepared under ultrahigh vacuum conditions by chemical vapor deposition using disilane and digermane as source gases. These gases offer a high sticking probability, and are suitable for atomic layer epitaxy. Using synchrotron radiation photoemission spectroscopy and scanning tunneling microscopy, we have examined the surface processes associated with the heteroepitaxial growth of Ge/Si. The measured surface-induced shifts and chemical shifts of the Si 2*p* and Ge 3*d* core levels allow us to identify the surface species and to determine the surface chemical composition, and this information is correlated with the atomic features observed by scanning tunneling microscopy. Issues related to precursor dissociation, attachment to dangling bonds, diffusion, surface segregation, growth morphology, and pyrolytic reaction pathways will be discussed. © *1997 American Vacuum Society.* [S0734-2101(97)07003-6]

I. INTRODUCTION

Preparation of Si-Ge interfaces by vapor deposition under ultrahigh vacuum (UHV) conditions is a subject of considerable interest to fundamental thin film science. These interfaces represent a simple ''prototypical'' system involving two elemental materials with similar physical and chemical properties, and yet a variety of interesting effects are expected because (1) the large lattice mismatch between Si and Ge causes strain in the overlayer, which is likely to affect the film morphology; and (2) Ge has a lower surface energy than Si, and therefore there is a tendency for Ge to segregate to the surface. Films of Si and Ge and their alloys are useful for a variety of electronic and optoelectronic device applications, and a detailed understanding of the atomistics of the growth is important for the engineering of interface structure and properties.

The present article discusses the atomic processes associated with UHV chemical vapor deposition (CVD) growth of Si and Ge films. The gases employed in this study are Si_2H_6 (disilane) and Ge_2H_6 (digermane).[1–16] These gases have low decomposition activation energies, and a high growth rate can be achieved at fairly low growth temperatures. The techniques employed in this study include photoemission spectroscopy and scanning tunneling microscopy (STM). Photoemission spectra of the Si and Ge core levels show surface-induced shifts and chemical shifts caused by bonding to hydrogen. A measurement of the relative intensities of the various surface components provides a chemical analysis of the surface. This information allows one to address questions such as which atoms (Ge or Si) are on the surface, and whether or not these surface atoms are bonded to hydrogen. STM, on the other hand, allows direct viewing of the surface atomic structure and morphology, and thus provides complementary information. Previous studies employing temperature programmed desorption, infrared spectroscopy, electron energy loss, and other techniques have yielded additional information regarding the desorption temperatures and the chemical species on the surface.[1–13] All of the available information together yields a detailed atomistic description of the pyrolytic reactions and growth behaviors.

Our experimental approach is to expose the surface to the CVD gas with the substrate typically held at room temperature. The sample is then annealed for a fixed period of time (60 s), and allowed to cool down before examination. This cycle is repeated for increasing annealing temperatures, and the results reveal the chemical reactions and atomic processes occurring in different temperature ranges. For Ge deposition on Si(100) and Si deposition on Ge(100), the initial sticking coefficient is high, and the coverage quickly saturates at about one-half of a monolayer (ML). After a high temperature anneal to drive off all of the surface hydrogen, the net deposition is $\sim 1/2$ ML. This quantized deposition can be repeated to build up a film with a precisely controllable thickness, and this process is known as atomic layer epitaxy.

The desorption temperatures of hydrogen from Si and Ge surfaces are significantly different because of a difference in bond energy. This difference may cause a transfer of hydrogen between Si and Ge upon annealing if both kinds of atoms are present on the surface. The interplay of surface energy, strain energy, and bond energy results in a variety of interesting effects that can be observed and studied in detail by photoemission and STM. It is not surprising that there are significant differences in the growth behaviors between Si on Ge and Ge on Si. Significant differences are also observed between the (100) and (111) faces,[16] although our discussion will be mainly for the (100) results due to space limitations.

[a)]Electronic mail: t-chiang@uiuc.edu

II. EXPERIMENTAL TECHNIQUES

Our STM measurements involve two instruments. One is homemade, and the other is an Omicron variable-temperature STM. Large-area scans that will be discussed below were generally low-pass filtered to remove a background in order to enhance the local features. These pictures resemble landscapes with oblique light illumination from the left. Atomic steps appear either bright or dark depending on the step direction. Atomic-resolution pictures over smaller areas are unaffected by this filtering, and bright parts simply represent protrusions. The photoemission measurements were carried out at the Synchrotron Radiation Center in Stoughton, Wisconsin, and at the Synchrotron Radiation Research Center in Hsinchu, Taiwan. The same sample preparation procedure was employed in all of these separate measurements. Commercial Si and Ge wafers were used. The Si samples were cleaned by flash heating to about 1400 K, whereas the Ge samples were cleaned by repeated cycles of sputtering by Ar ions followed by annealing. After cleaning these surfaces exhibited sharp electron diffraction patterns. Digermane, diluted to 20% in He, and pure disilane were used for CVD growth. The ion gauge readings were corrected for the sensitivity to these gases. Heating of the sample was done by passing a current through the sample itself, and the temperature of the sample as a function of heating power was calibrated by attaching a small thermocouple to the center of the back face of an identical test sample.

Figure 1(a) shows a typical Si $2p$ core level spectrum taken from a clean Si(100)-(2×1) surface. The line shape can be divided into three major components B (''bulk''), S' (surface component 1), and S (surface component 2) as shown in Fig. 1(a), where each component consists of a pair of spin-orbit-split peaks. The peak on the lower binding energy side in Fig. 1(a) is the $2p_{3/2}$ peak of the S component. It is well separated from the rest of the line shape, and its intensity can be deduced by fitting. This component is associated with the dimer atoms on the (2×1) reconstructed surface, as was demonstrated in previous studies.[17,20] The intensity of the unresolved S' component cannot be easily deduced, and will not be used in this study.

If the Si(100) surface becomes partially covered by Ge or H, the S component will diminish, and its intensity is a quantitative measure of the surface area that remains clean. Shown in Fig. 1(b) is a spectrum of Si(100) covered by 4.5 ML Ge prepared by molecular beam epitaxy (MBE). Only the B component remains in the spectrum. This is because the bonding between Si and Ge is very similar to that between Si and Si, and as a result, all Si atoms under such a thick layer of Ge are in a bulklike bonding environment. If the Si(100) surface is terminated by hydrogen, the core level spectrum will show hydrogen-induced chemical shifts to higher binding energy, as illustrated in Fig. 1(c).[15] The S component characteristic of the clean surface is not present. If the hydrogen is then driven off the surface by thermal annealing, the hydrogen-induced component will diminish, and the S component will reappear. A measurement of the core level line shape thus provides a chemical analysis of the surface.

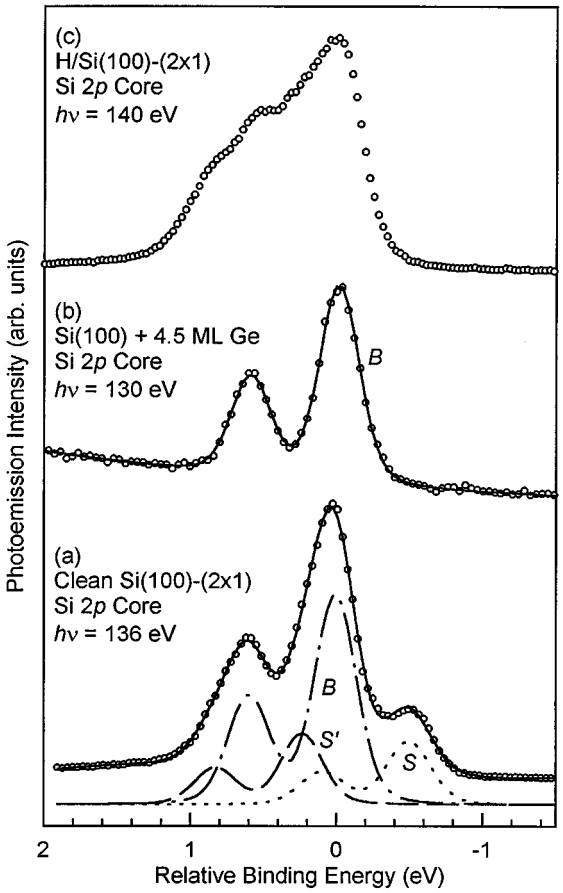

FIG. 1. Photoemission spectra for the Si $2p$ core level taken from (a) clean Si(100)-(2×1), (b) Si(100) covered by 4.5 ML of Ge prepared by MBE, and (c) a monohydride-terminated Si(100) surface. The circles are data points, and the solid curves are fits to the data. The fits involve three components (B, S', and S) for (a), and one component (B) for (b).

The Ge $3d$ core level spectrum taken from clean Ge(100)-(2×1) shows a line shape very similar to Si(100). There are again three major components, B, S', and S, where the S component, shifted to lower binding energies, can be associated with the dimers on the surface. This surface also shows a hydrogen-induced chemical shift. In our experiments, both the Si and Ge core level line shapes are measured.

STM and electron diffraction reveal the surface symmetry. An observed (2×1) reconstruction implies the presence of either Si or Ge dimer bonds on the surface, even though the dimer dangling bond could be terminated by either a H or a SiH_3 (GeH_3) group. A surface terminated by SiH_2 (GeH_2) exhibits a local (1×1) structure.

III. RESULTS AND DISCUSSION

A. Adsorption and pyrolytic reactions for Si on Ge(100)

The results from all available experimental studies can be summarized by the following pyrolytic reactions for disilane adsorbed on Ge(100) for increasing substrate temperatures:

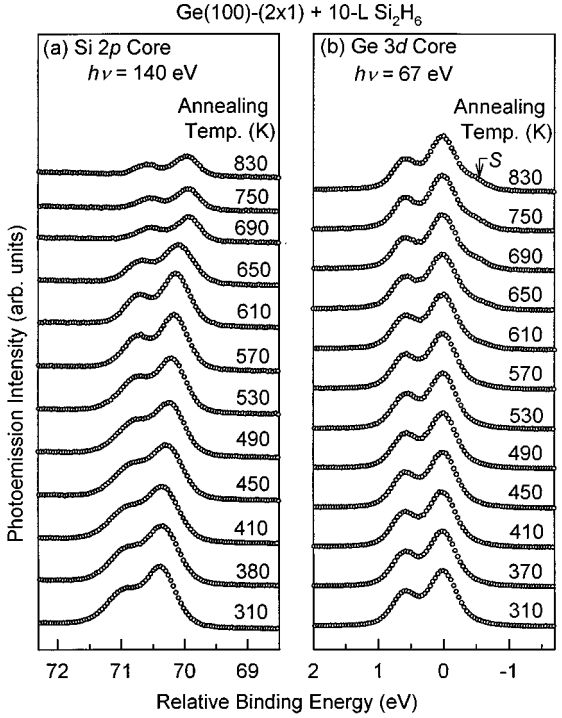

FIG. 2. Photoemission spectra for (a) Si 2*p* and (b) Ge 3*d* core levels for various annealing temperatures as indicated. The sample is Ge(100) initially saturated by a 10 L disilane exposure at RT.

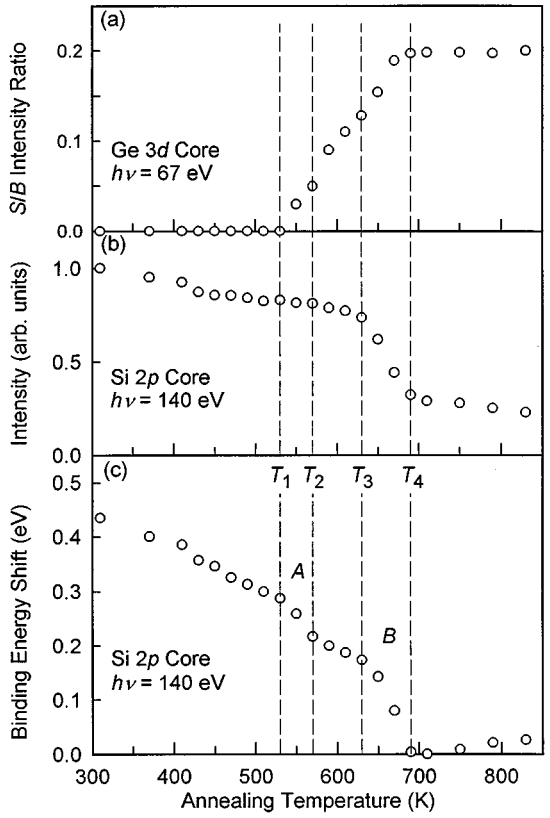

FIG. 3. (a) Intensity ratio of the *S* and *B* components of Ge 3*d*, (b) integrated intensity of Si 2*p*, and (c) binding-energy shift of the Si 2*p* as a function of annealing temperature. The sample is Ge(100) initially saturated by a 10 L disilane exposure at RT. Two temperature ranges, *A* and *B*, and four temperatures, T_1-T_4, associated with the reactions are indicated.

$$Si_2H_6(g)\rightarrow 2SiH_3(s) \quad (RT), \tag{1}$$

$$SiH_3(s)+Ge(s)\rightarrow SiH_2(s)+GeH(s) \quad (RT-530\ K), \tag{2}$$

$$GeH(s)\rightarrow Ge(s)+1/2H_2(g) \quad (530-620\ K), \tag{3}$$

$$SiH_2(s)+SiH_2(s)\rightarrow Si_2H_2(s)\ (\text{monohydride dimer}) + H_2(g) \quad (530-570\ K), \tag{4}$$

and

$$Si_2H_2(s)\rightarrow 2Si(b)+H_2(g) \quad (630-690\ K). \tag{5}$$

In these equations, (s), (b), and (g) refer to a surface species, an atom in the substrate below the surface, and a gas molecule, respectively. The approximate temperature range for each reaction is indicated, and RT refers to room temperature.

We will now examine the experimental evidence. Figure 2 shows Si 2*p* and Ge 3*d* core level spectra for various annealing temperatures starting from a Ge(100)-(2×1) surface saturated by disilane exposure at RT. The evolution of the main features as a function of annealing temperature is summarized in Fig. 3. Figure 3(a) is a plot of the intensity ratio between the *S* and *B* components of the Ge 3*d* core level, which is an indication of the surface area that is clean Ge(100)-(2×1). Figure 3(b) is a plot of the intensity of the Si 2*p* core, where the significant drop in intensity indicates Si indiffusion. Figure 3(c) shows the binding energy shift of the Si 2*p* core level, which reflects chemical shifts as well as band bending shifts caused by a change in surface chemical composition. Four characteristic temperatures $T_{1-4}=530$, 570, 630, and 690 K and two transitions *A* (between T_1 and T_2) and *B* (between T_3 and T_4) are indicated in the Fig. 3.

Figure 4 shows a 210×250 Å^2 STM picture for 0.02 langmuir (L) exposure at RT. Randomly distributed adsorption sites are observed. Several possible bonding configurations for the molecular fragments are shown in Fig. 5. Configuration A corresponds to two SiH_3 bonded on the same side of two neighboring dimers, resulting in an elongated bright protrusion located on one side of the two affected dimers. This is the dominant configuration found in our STM pictures. Configuration B involves the same two fragments bonded on the two dangling bonds of a single dimer. A very small fraction of the adsorption sites is characterized by configuration C shown in Fig. 5. Again, two neighboring dimers are involved, and the images show a bright protrusion centered about the dimer row. This can be identified as two SiH_2 with a local (1×1) structure; these SiH_2 fragments are formed as a result of the decomposition of SiH_3 as indicated by Eq. (2). Configuration D in Fig. 5 corresponds to a monohydride dimer. This configuration is observed only after the sample has been annealed to higher temperatures. Note that the monohydride dimer has a local (2×1) structure similar to the dimer on the clean surface.

For all of these RT adsorption configurations (A, B, and C), the two fragments of dissociative chemisorption occupy

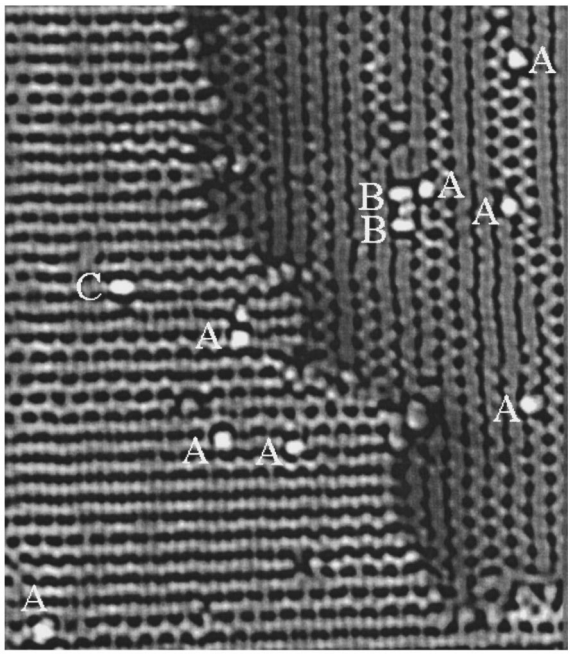

FIG. 4. A STM image of Ge(100)-(2×1) dosed by 0.02 L of disilane at RT. The area is 210×250 Å^2.

neighboring dangling bond sites, and this has an important implication. The initial sticking coefficient for disilane on Ge(100)-(2×1) is ~0.5 from our STM measurements. For the same experiment on the Ge(111)-c(2×8) surface, the sticking coefficient is reduced by three orders of magnitude.[16] This drastic difference can be related to the fact that two nearby Ge dangling bonds are needed for the dissociative chemisorption, and the distance between the two dangling bonds must match the Si-Si distance in Si_2H_6 to facilitate the dissociation. This condition is well satisfied for the Ge(100) surface, but not for the Ge(111)-c(2×8) surface, for which neighboring dangling bonds on the surface are separated by much larger distances due to the c(2×8) reconstruction.[16]

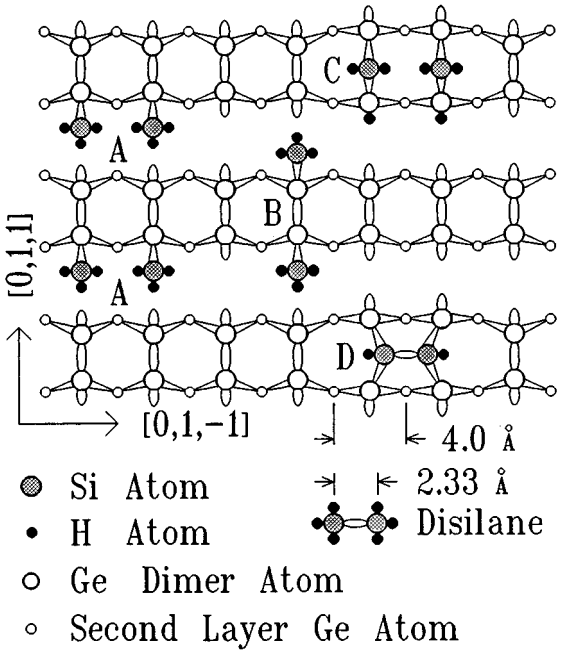

FIG. 5. Schematic diagrams for various bonding configurations of disilane fragments on Ge(100)-(2×1).

As the exposure increases, more dissociative chemisorption fragments are observed, and the surface becomes saturated for exposures greater than a few langmuirs. Because the pairs of dangling bonds involved in different adsorption events are not necessarily phase correlated, the resulting saturated surface appears disordered as seen by STM. Reflection high-energy electron diffraction from the same surface, however, shows a (2×1) pattern, indicating that many of the dimer bonds underneath the disordered adlayer remain intact (care was taken to avoid surface modification by electron beam irradiation). This is consistent with the STM results mentioned above that most fragments after a low exposure are SiH_3.

As the annealing temperature increases, these SiH_3 fragments dissociate into SiH_2 according to Eq. (2). This covers a wide temperature range as indicated by Fig. 3(b), which shows a continuous change of the Si 2p binding energy. The adlayer remains disordered. Transition A between T_1 and T_2 is characterized by desorption of H from SiH_2, long-range diffusion of surface fragments to form monohydride islands, and desorption of H from GeH. After a 620 K anneal, these processes are complete, and the surface is left with about 1/2 ML of silicon monohydride islands on an otherwise clean Ge(100)-(2×1) surface, as seen in Fig. 6(a), which is a 500×500 Å^2 STM picture. We know from the (2×1) dimer reconstruction that these islands are in the form of silicon monohydride. We also know that the part of the surface not covered by these islands is clean Ge(100)-(2×1) because the intensity of the S component of the Ge core level has recovered to about one-half of the value for the clean surface, as seen in Fig. 3(a).

Further annealing leads to transition B indicated in Fig. 3. The SiH islands lose H based on desorption measurements, and as soon as the H leaves, the Si left behind diffuses into a subsurface site because of the lower surface free energy of Ge relative to Si. This indiffusion is evidenced by the large drop in intensity of the Si 2p core level seen in Fig. 3(b), which is accompanied by a large shift in binding energy seen in Fig. 3(c). Simultaneously, the intensity of the S component of the Ge core level recovers to the clean surface value, as seen in Fig. 3(a). Thus, the final configuration after transition B is one in which all of the hydrogen is desorbed, the top layer is Ge, and the 1/2 ML of Si derived from the adsorbed Si_2H_6 is in the subsurface region. Figure 6(b) is an STM picture showing the (2×1) reconstruction of the top Ge layer.

It is interesting to note that Si indiffusion is correlated with the desorption of H from SiH. This is contrasted by the observed Si indiffusion at much lower temperatures during MBE growth of Si on Ge.[21] Apparently, the presence of H

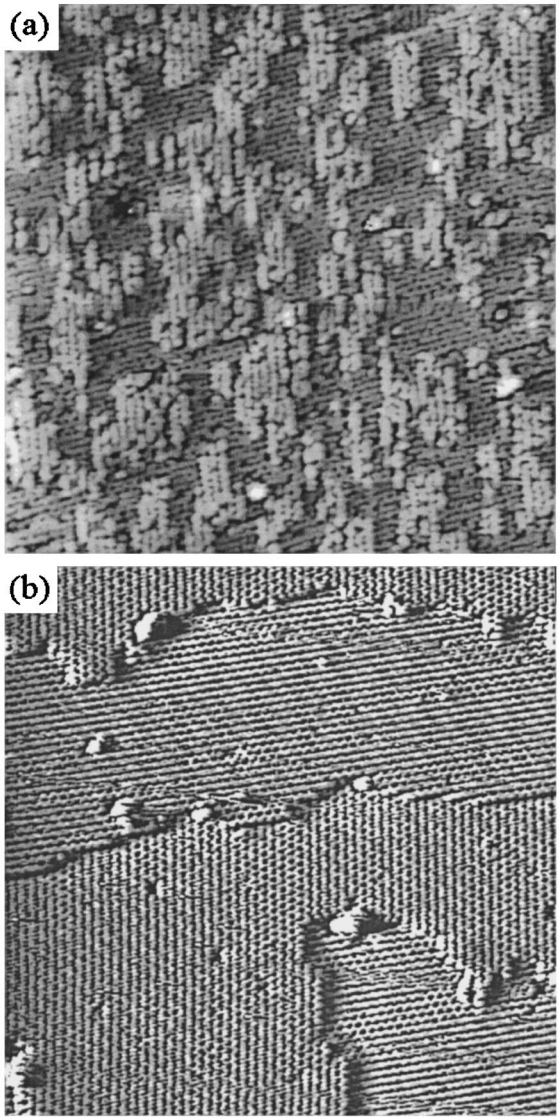

FIG. 6. 500×500 Å^2 STM images for Ge(100)-(2×1), saturated with a 5 L disilane dose at RT, and then annealed to (a) 620 and (b) 720 K.

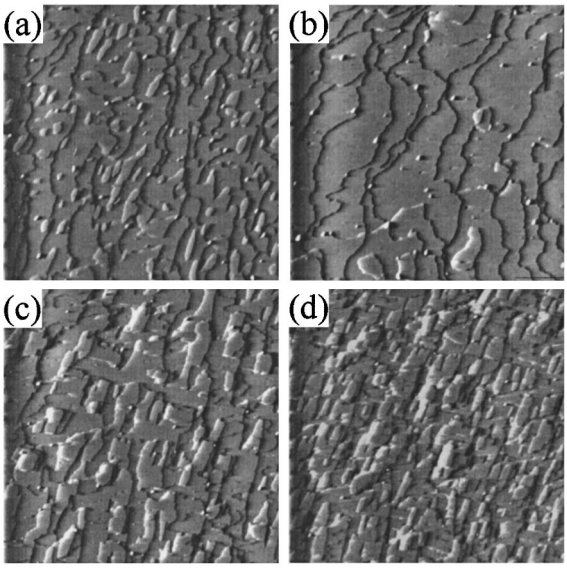

FIG. 7. 4000×4000 Å^2 STM images of Ge(100)-(2×1), saturated with a 5 L disilane dose at RT, and then annealed to (a) 720 and (b) 820 K. (c),(d) The same scale images of Ge(100) after (c) 5 and (d) 10 cycles of Si growth. Each cycle involves an exposure of 5 L disilane at 340 K followed by annealing at 820 K.

bonded to Si in the CVD case hinders the indiffusion of Si. Another interesting effect is that the H desorption temperature from the SiH islands on Ge(100) observed in this experiment is significantly lower than the desorption temperature of H from the Si surface. This may be explained by a concerted motion involving Si, Ge, and H, or a mechanism involving the diffusion of H from the SiH islands onto a nearby exposed Ge surface where the H atoms can be readily desorbed because of the lower desorption temperature of H from GeH.

Some recent results have suggested that a mixed Si–Ge dimer layer consisting of Si atoms in the down dimer position and Ge atoms in the up dimer position might be energetically or kinetically more favorable under certain growth conditions in the preparation of Si–Ge interfaces.[20,22] Our results show clearly that this is not the case for the system under study. If the Si atoms merely move into the down dimer positions, there would be little reduction in the Si core level intensity, in disagreement with the data in Fig. 3(b). Even though the measured core level intensity can be somewhat affected by diffraction effects,[23] the intensity reduction is so large that these Si atoms cannot all reside in the layer just below the dimer layer. Some of the Si atoms must have moved into deeper layers. This is consistent with recent transmission electron microscopy (TEM) results which show that Si growth on Ge by MBE at similar temperatures results in an intermixed interface.[24]

Further annealing to even higher temperatures results in a further and gradual reduction of the Si core level intensity, indicating that the Si atoms are moving farther below the surface. Figures 7(a) and 7(b) show the surface morphology after a 720 and 820 K anneal, respectively, over a 4000 ×4000 Å^2 area. The islands seen in Fig. 7(a) are mostly absorbed by the steps with increasing annealing temperatures, but it is difficult to eliminate all islands. Figure 7(b) shows some remaining islands that should have been absorbed by the step edges based on diffusion length considerations. This seems strange, but it can be explained by surface strain caused by the lattice mismatch between Si and Ge. Figures 7(c) and 7(d) show the surface morphology after 5 and 10 cycles of atomic layer epitaxy, where each cycle involves saturating the surface with disilane at room temperature followed by annealing to 820 K. The effect of strain becomes clear now; the surface becomes covered by multilayer islands and holes to minimize the buildup of long-range strain. The lateral length scale becomes smaller as more growth cycles are performed. Detailed STM images show that the surface remains (2×1) everywhere including the top of the islands and the bottom of the holes.

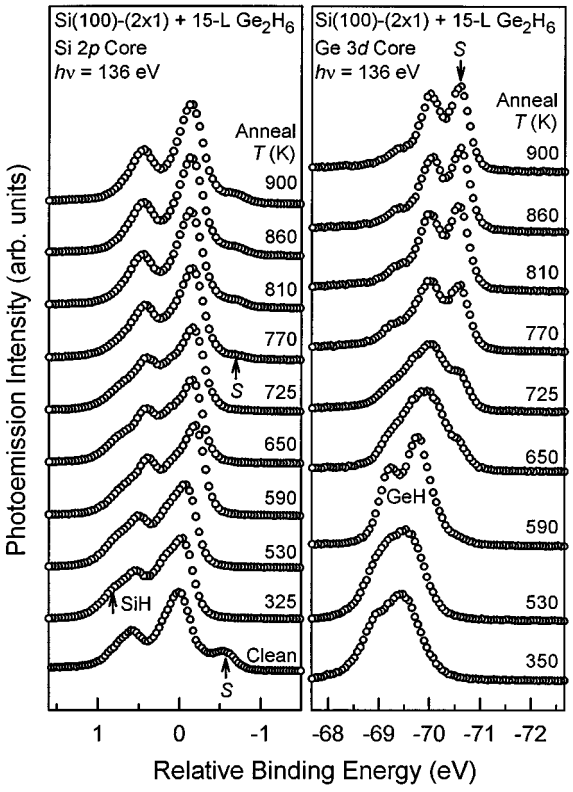

FIG. 8. Photoemission spectra for Si 2*p* and Ge 3*d* core levels for various annealing temperatures as indicated. The sample is Si(100) initially saturated by a 15 L digermane exposure at 325 K.

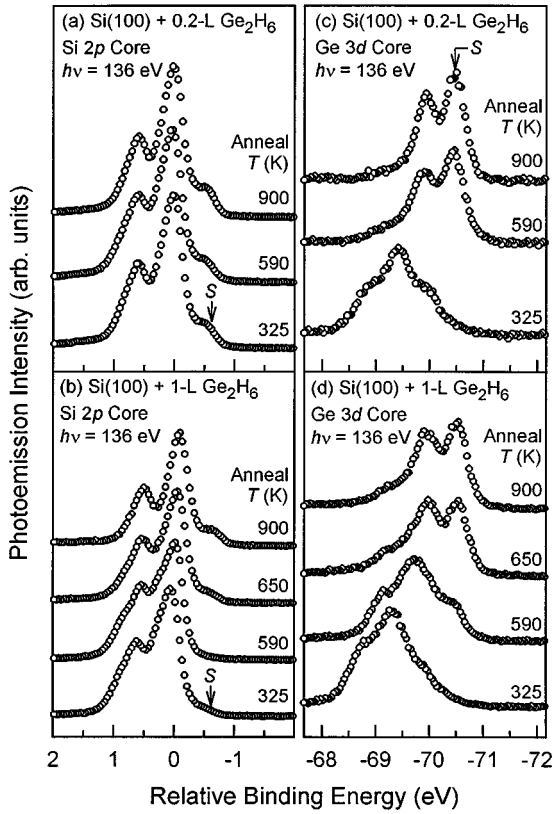

FIG. 9. (a),(b) Photoemission spectra of Si 2*p* at various annealing temperatures for an initial digermane exposure of 0.2 and 1.0 L, respectively. (c),(d) The corresponding Ge 3*d* core level spectra.

B. Adsorption and pyrolytic reactions for Ge on Si(100)

The initial sticking coefficient of digermane on Si(100) is again about 0.5, and the surface becomes saturated after an exposure of a few langmuirs. It might be expected that the annealing behavior of the digermane-saturated Si(100) surface should be generally similar to the case of Si on Ge(100), and it is indeed the case based on our experiment. One important difference is that the Ge remains on the surface after a high temperature anneal to desorb all H. In other words, the indiffusion of Si observed in the previous case has no counterpart for Ge growth on Si(100). Figure 8 shows the Si and Ge core level line shapes as a function of annealing temperature for a Si(100) surface initially saturated by digermane exposure. The Ge 3*d* line shape for the initial surface is broad because the Ge is in the form of a mixture of various hydrides. After annealing to 590 K, the line shape sharpens into that of GeH. The H is desorbed at even higher annealing temperatures, and the final Ge line shape consists of one major component, the *S* component, corresponding to Ge in the top dimer layer. The Si line shape in Fig. 8 shows that the *S* component is eliminated by the adsorption, and partially recovers for annealing temperatures higher than 770 K due to the desorption of H.

A very interesting coverage-dependent effect is observed. Figure 9 shows a comparison between two different initial digermane exposures, 0.2 and 1 L. The Ge core level spectra in Fig. 9(c) indicate that the conversion of Ge hydrides into surface Ge becomes complete at 590 K for an initial exposure of 0.2 L. Figure 9(d) shows that the same conversion does not become complete until 650 K for an initial exposure of 1 L. The results in Fig. 8 further show that this conversion does not become complete until an even higher temperature of 770 K for a fully saturated surface. The explanation for this variation in temperature as a function of initial coverage is that the decomposition of GeH proceeds via two pathways: (1) H_2 desorbs directly from a monohydride dimer Ge_2H_2, and (2) a lower-temperature process in which the H atoms are transferred from GeH to nearby Si surface atoms to form SiH. The latter process is possible because the Si–H bond is stronger than the Ge–H bond as already noted above, but will require nearby Si dangling bonds, which are more abundant at lower digermane exposures. For higher initial digermane exposures, process (2) becomes suppressed due to the lack of available Si dangling bonds, leading to a higher temperature for the conversion of GeH into surface Ge. Figures 9(a) and 9(b) show the corresponding Si core level spectra. When H is transferred from GeH to Si during the annealing, one would expect the intensity of the *S* component of the Si core level to drop, and this is indeed observed. In Figs. 9(a) and 9(b), the *S* intensity of Si decreases initially due to this effect, and increases at higher annealing temperatures when H is desorbed from Si.

STM observations show that the room-temperature satu-

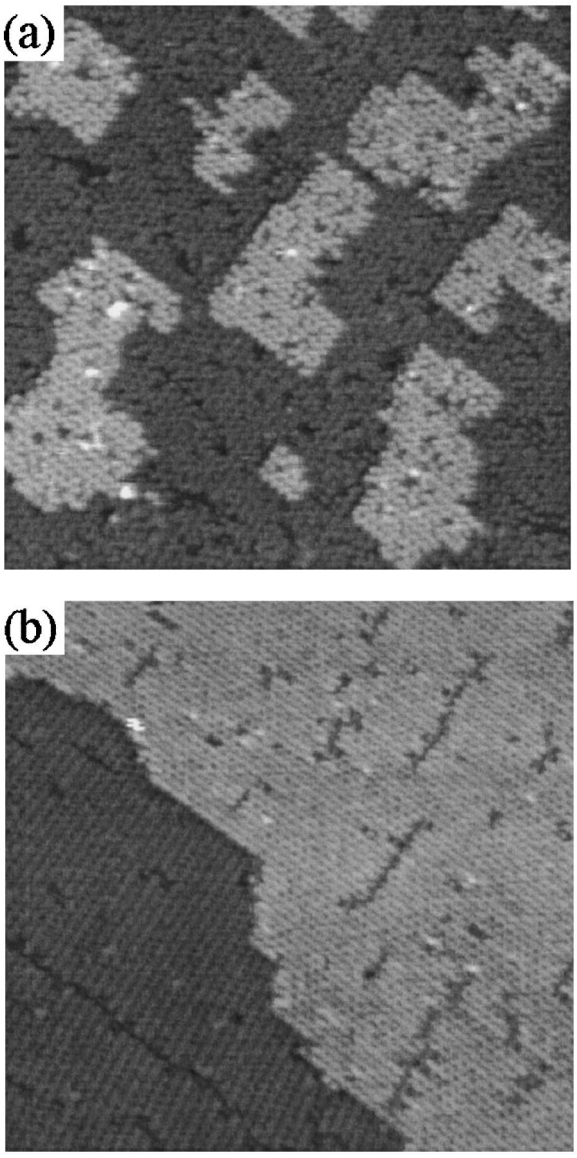

FIG. 10. 450×450 Å^2 STM images of Ge(100)-(2×1), exposed to 5 L disilane at RT, and then annealed to (a) 810 and (b) 900 K.

rated surface is disordered as in the previous case. Figure 10 (a) is a picture taken after annealing to 810 K. Here, one sees (2×1) islands covering roughly one-half of the surface. At this annealing temperature, there is very little H left on the surface. Annealing to an even higher temperature of 900 K causes the islands to coarsen and attach to step edges. This is illustrated in Fig. 10(b). Dimer rows interrupted by missing dimer defects are observed, and these defects tend to form rows perpendicular to the dimer rows. This is caused by strain, and the results are very similar to the $(2\times n)$ reconstructions reported by other groups for the MBE growth of Ge on Si.[22,25] This is not surprising, since at temperature high enough for complete H desorption, the growth should be similar for CVD and MBE. In contrast to the case of Si on Ge, the growth of Ge on Si is characterized by a fairly abrupt interface.[24] In both cases, the resulting morphology after multi-layer growth is three dimensional because of the strain.[22]

IV. CONCLUSIONS

A combined spectroscopy and microscopy study can yield detailed information about surface atomic processes as demonstrated in this study. The growth of Si/Ge interfaces represents one of the simplest CVD processes, and yet it is clear from the above discussion that the growth can involve a variety of interesting effects and phenomena. The interplay of precursor molecular structure, surface reconstruction, surface energy, bond energy, and strain can result in complex surface morphologies and nontrivial chemical compositions near the surface. This work provides a basis for understanding many of the generic features of hydrogen chemistry of semiconductor surfaces, pyrolytic reactions, and heteroepitaxial growth by CVD.

ACKNOWLEDGMENTS

This material is based upon work supported by the National Science Council, Republic of China, under Contract Nos. NSC84-2112-M009-031 and NSC85-2112-M009-024 (D.S.L.), and by the U.S. Department of Energy (Division of Materials Sciences, Office of Basic Energy Sciences), under Grant No. DEFG02-91ER45439 (T.C.C.). An acknowledgment is also made to the Donors of the Petroleum Fund, administered by the American Chemical Society, and to the U.S. National Science Foundation (Grant Nos. DMR-95-31809 and 95-31582) for partial support of the beamline operation at the Synchrotron Radiation Center. The Synchrotron Radiation Center is supported by the U.S. National Science Foundation under Grant No. DMR-95-31009.

[1]F. Bozso and Ph. Avouris, Phys. Rev. B **38**, 3943 (1988).
[2]D. Lubben, R. Tsu, T. R. Bramblett, and J. E. Greene, J. Vac. Sci. Technol. A **9**, 3003 (1991).
[3]H. Hirayama, T. Tatsumi, and N. Aizaki, Appl. Phys. Lett. **52**, 1484 (1988).
[4]S. M. Gates, Surf. Sci. **195**, 307 (1988).
[5]R. Imbihl, J. E. Demuth, S. M. Gates, and B. A. Scott, Phys. Rev. B **39**, 5222 (1989).
[6]S. M. Gates and C. M. Chiang, Chem. Phys. Lett. **184**, 448 (1991).
[7]J. J. Boland, Phys. Rev. B **44**, 1383 (1991).
[8]Y. Suda, D. Lubben, T. Motooka, and J. E. Greene, J. Vac. Sci. Technol. A **8**, 61 (1990).
[9]N. Ohtani, S. M. Mokler, M. H. Xie, J. Zhang, and B. A. Joyce, Surf. Sci. **284**, 305 (1993).
[10]B. M. Ning and J. E. Crowell, Appl. Phys. Lett. **60**, 2914 (1992); Surf. Sci. **295**, 79 (1993).
[11]C. Isobe, H.-C. Cho, and J. E. Crowell, Surf. Sci. **295**, 117 (1993).
[12]D.-A. Klug, W. Du, and C. M. Greenlief, J. Vac. Sci. Technol. A **11**, 2067 (1993); Chem. Phys. Lett. **67**, 2187 (1991).
[13]M. J. Bronikowski, Y.-W. Wang, M. T. McEllistrem, D. Chen, and R. J. Hamers, Surf. Sci. **298**, 50 (1993).
[14]D.-S. Lin, E. S. Hirshorn, T.-C. Chiang, R. Tsu, D. Lubben, and J. Greene, Phys. Rev. B **45**, 3494 (1992).
[15]D.-S. Lin, T. Miller, and T.-C. Chiang, Phys. Rev. B **47**, 6543 (1993).
[16]D.-S. Lin, E. S. Hirshorn, T. Miller, and T.-C. Chiang, Phys. Rev. B **49**, 1836 (1994).

[17]D.-S. Lin, T. Miller, and T.-C. Chiang, Phys. Rev. Lett. **67**, 2187 (1991); J. E. Rowe and G. K. Wertheim, *ibid.* **69**, 550 (1992); F. J. Himpsel, *ibid.* **69**, 551 (1992); D.-S. Lin, J. A. Carlisle, T. Miller, and T.-C. Chiang, *ibid.* **69**, 552 (1992).
[18]X. Yang, R. Cao, J. Terry, and P. Pianetta, Phys. Rev. B **45**, 13749 (1992).
[19]E. Landemark, C. J. Karlsson, Y.-C. Chou, and R. I. G. Uhrberg, Phys. Rev. Lett. **69**, 1588 (1992).
[20]L. Pattey, E. L. Bullock, T. Abukawa, S. Kono, and L. S. O. Johansson, Phys. Rev. Lett. **75**, 2538 (1995).
[21]D.-S. Lin, T. Miller, and T.-C. Chiang, Phys. Rev. B **45**, 11 415 (1992).
[22]The chemical composition of the dimer layer for submonolayer Ge deposition on Si(100) remains an open question. See the discussion of F. Liu and M. G. Lagally, Phys. Rev. Lett. **76**, 3156 (1996).
[23]M. T. Sieger, D. A. Luh, T. Miller, and T.-C. Chiang, Phys. Rev. Lett. **77**, 2758 (1996).
[24]D. E. Jesson, S. J. Pennycook, and J.-M. Baribeau, Phys. Rev. Lett. **66**, 750 (1991).
[25]F. Wu and M. G. Lagally, Phys. Rev. Lett. **75**, 2534 (1995).